

Experimental study of gas adsorption using high-performance activated carbon: Propane adsorption isotherm

Tine Aprianti^{1,2}, Harrini Mutiara Hapsari³, Debby Yulinar Permata⁴, Selvia Aprilyanti⁵, Justin Sobey², Kallan Pham², Srinivasan Kandadai² and Hui Tong Chua^{2*}

¹ Department of Chemical Engineering, Faculty of Engineering, Universitas Sriwijaya, **INDONESIA**

² Department of Chemical Engineering, School of Engineering, The University of Western Australia, **AUSTRALIA**


³ Department of Architecture Engineering, Faculty of Engineering, Universitas Sriwijaya, **INDONESIA**

⁴ Department of Civil Engineering, Faculty of Engineering, Universitas Sriwijaya, **INDONESIA**

⁵ Department of Industrial Engineering, Faculty of Engineering, Universitas Tridini, **INDONESIA**

* Corresponding Author: huitong.chua@uwa.edu.au

Received December 21st 2023; 1st Revised May 06th 2024; 2nd Revised May 28th 2024; Accepted May 28th 2024

 Cite this <https://doi.org/10.24036/teknomekanik.v7i1.28672>

Abstract: Activated carbon is widely used for its diverse adsorptive abilities, with a vast range of current and emerging uses. This study developed a data set for high-performing activated carbon, its adsorption abilities with differing adsorbents, and an understanding of what deviations are present compared to the widely used adsorption models. This study included the construction of Tóth isotherms in varying conditions. Building a strong isotherm correlation is desired, with an understanding of the relationship between the pores of the activated carbon sample, operating parameters, and the adsorbent. The present data could complement efforts in designing adsorbed natural gas storage systems. Experimental data was collected using a Constant Volume Variable Pressure (CVVP) apparatus, consisting of a temperature-regulated vessel containing the activated carbon sample dosed with varying adsorbents through a controlled dosing vessel. Analysis of the derived data gave a well-fitted Tóth adsorption isotherm, giving the maximum specific adsorption capacity of the activated carbon to be 2.28 g of propane per gram of activated carbon with a standard error of regression $\hat{\sigma}$ of 0.01 g/g, and the experimental data are associated with 0.24% of uncertainty. The free space calculation from the helium calibration produced a value of 43.3 ± 0.7 cm³.

Keywords: Refrigeration cycle; Helium calibration; Thermodynamic; Industry, innovation and infrastructure

1. Introduction

Activated carbon is a substance widely used for its excellent adsorptive capabilities. Extensive microscopic pores in the material allow large volumes of fluids to adhere to it for a relatively small volume and mass of carbon. It is commonly used in chemical recovery and purification applications, air and odour scrubbing, clean-up operations, and poison treatments. An application that is a research topic is adsorption refrigeration, which has the benefit of vibration- and electricity-free refrigeration. The propane usage in domestic refrigerators is examined in terms of energy consumption, compressor lubrication, costs, availability, environmental factors, and safety. It is concluded that propane is an attractive and environmentally friendly alternative to CFCs used [1].

This experiment examines the adsorption behaviour of propane on a sample of Maxsorb II activated carbon. The apparatus consists of CVVP vessels placed in temperature-controlled water baths to maintain thermal stability. The free expansion between the CVVP vessels was used to measure state changes of the contained gas. Data on propane adsorption was gathered, and a Tóth adsorption isotherm was accurately fitted to the data. The CVVP apparatus setup allows for the construction of isotherms, tracking adsorbates behaviour and adsorption capabilities under varying pressures and temperatures. Previous work has looked at the calibration of the experimental apparatus using helium; this study only performed helium calibration without further experiments using propane or other gases [2]. Another study was conducted to investigate the adsorption characteristics of methane on a Maxsorb II specimen of activated carbon that was measured over the temperature range of (281 to 343) K and at pressures up to 1.2 MPa using a new volumetric measurement system [3]. The results of the methane study are shown in Figure 1.

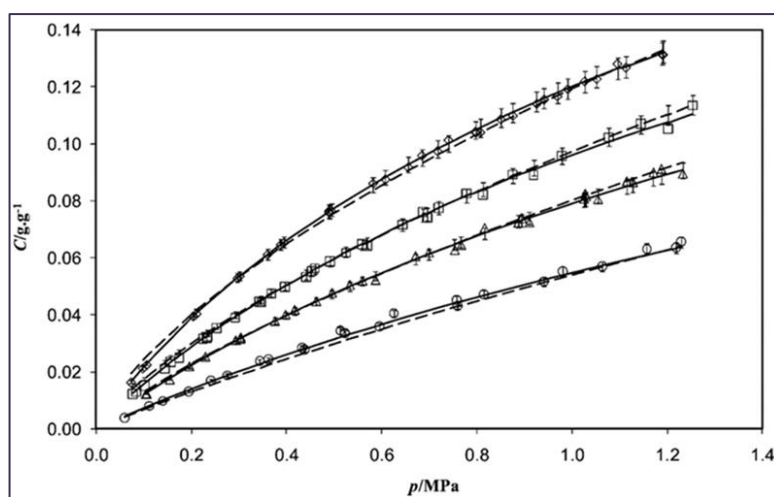


Figure 1. Methane adsorption isotherms on Maxsorb II at 281 K, 298 K, 313 K, and 343 K with Toth and Dubinin-Astakhov isotherms [3]

Current uses of activated carbon include filtration to create drinking water, ingestion to treat poisoning by preventing the uptake of poisons into the victim, treating air pollution, and purifying other liquids and gases [4], [5], [6], [7], [8], [9]. The high surface area of activated carbon allows it to perform well in these filtration and extraction roles based on its adsorptive capabilities. Future uses include the adsorption refrigeration cycle and replacing the mechanical compressor with a thermal compressor. A diagram of the adsorption refrigeration cycle is shown in Figure 2. The thermal compressor consists of two vessels containing an adsorbent, one saturated with the adsorbate refrigerant and the other dry. The saturated vessel is heated, allowing endothermic desorption to occur, and is termed the desorption vessel. The off-gassing refrigerant leaves the desorption vessel to flow through the condenser, expander, and evaporator before it reaches the dry adsorption vessel. The adsorption vessel adsorbs the refrigerant, allowing the fluid to flow around the system in a pseudo-closed cycle and then releases the heat of adsorption, which is cooled by the environment.

There are some possible adsorbate/adsorbent pairs, of which activated carbon and propane are one, with examples of other pairs, such as methyl alcohol as adsorbate and silica gel as adsorbent [10]. Activated carbon can be produced physically or chemically. Physical production usually involves carbonising: carbon-rich materials such as wood, bamboo, crop husks, peat, or coal are heated up to 2000°C until 20-39% of the original mass remains [4], [11], [12]. This is like cooking, leaving a carbon structure with the volatiles burnt off. Chemical production involves submerging the carbon-rich source in acid, base, or salt at 450-900°C [5], [6], [7], [8], [13], [14], [15]. This process is generally more commercially viable due to the lower temperature.

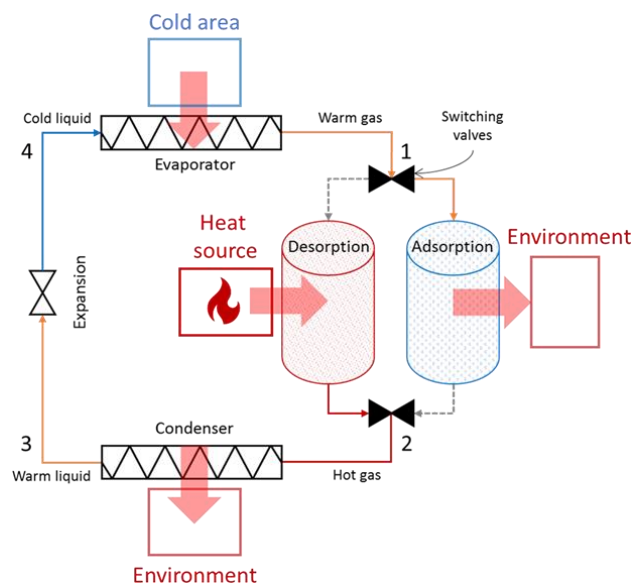


Figure 2. Diagram of a simple adsorption refrigeration cycle

Activated carbon has some parameters that are used to characterise its performance. Iodine Number is used to measure the performance of activated carbon at adsorbing small molecules sized up to 2 nm (micropores). It is defined by the number of milligrams of iodine adsorbed per gram of activated carbon, which typically ranges from 500-1000 mg/g [7]. BET Surface Area uses the BET model to measure the porosity of the activated carbon available for nitrogen adsorption at its boiling point [16]. Activated carbon can have a BET surface area of 3000 m²/g [5]. Methylene blue is a measure of the ability of activated carbon to adsorb particles sized 2 nm to 5 nm (mesopores), such as methylene blue. It is given as grams of methylene blue per 100 g of activated carbon, with typical values of 12-30 g/100 g [12].

Propane as refrigerant R290 was a popular natural refrigerant until the 1920s, before the discovery and widespread use of CFCs. Freon (R-12) was a popular CFC refrigerant, the first non-flammable, non-toxic refrigerant [17]. When the high ozone-damaging potential of CFCs was discovered in the 1980s, it led to the enactment of the Montreal Protocol and the eventual banning of CFCs and HCFCs. To fill this gap, HFCs, such as the ubiquitous R134a, which have a minimal impact on the ozone layer, became widely used but were later found to have enormous global warming effects. This led to the enactment of the Kyoto Protocol, which came into force in 2005 and has begun efforts to phase out HFCs to reduce the greenhouse effect and global warming.

Before using R-12, propane was described as an “odourless safety refrigerant” [17]. This demonstrates the danger of early refrigerants, which were commonly flammable, highly toxic, or both. No modern refrigerants can satisfy the ideal trade-offs of low toxicity and flammability with no long-lasting environmental damage in the upper atmosphere while still having viable operating conditions. The flammability of propane is an issue, but with many other refrigerants being banned, the use of propane as a refrigerant has again increased.

Propane is also an easily transportable fuel for vehicles and heating in the form of Liquefied Petroleum Gas (LPG). LPG is stored as a mixture of propane and butane as a liquid at room temperature using high pressure. Activated carbon or other microporous materials are an attractive option for improving propane storage. By adsorption, pressure vessels containing activated carbon can store a larger gas mass at a lower pressure [5].

Propane and butane have different boiling points. Propane can handle much lower temperatures, so it is used in homes with outdoor storage. Butane is better stored indoors as it does not function

as effectively in colder climates [18], [19], [20]. Propane is usually obtained from wet natural gas production. The reservoirs from where the hydrocarbons are obtained can contain impurities such as sulphur, which can cause corrosion issues with pipelines, pressure vessels, and heat exchangers [21]. Combustion products of these impurities, such as sulphur oxides, are hazardous environmental pollutants and pose health risks, which can also damage catalytic converters designed to reduce vehicle emissions [22]. Activated carbon is a good candidate for filtering these impurities and creating cleaner storage, transport, and combustion gas.

Different models for adsorption sites use different adsorption assumptions, such as monolayer adsorbates, where only a single layer of adsorbate molecules is deposited on the adsorbent, which has a homogenous distribution of adsorption sites. The pressure of the gas is much lower than its saturation pressure. Multilayer adsorbates can adhere to already adsorbed molecules, creating stacked adsorbate layers. The adsorption energy of each subsequent layer decreases. The pressure of the gas approaches its saturation pressure in the system. Pore fluids, where the adsorbent has cylindrical adsorption sites of finite diameter that can gradually be filled with adsorbed molecules. Molecules larger than the pore diameter cannot adhere to these sites [2], [19]. The Freundlich isotherm is a purely empirical isotherm model developed by Freundlich and Kuster in 1906. The formula is described by [23]:

$$\theta = kP^n \quad (1)$$

where θ is the mass ratio between adsorbate to adsorbent, k , and n are the empirical constants for the gas-adsorbate pair, and P is the pressure of the adsorbing gas.

The Langmuir isotherm was developed by Irving Langmuir in 1918. The model assumes a monolayer adsorbate with an ideal gas without interaction between molecules. The model is defined by Eq. 2.

$$\theta = \frac{Kp}{1 + Kp} \quad (2)$$

θ is the proportion of adsorption sites occupied, K is the sorption equilibrium constant, and p is the partial pressure of the gas [24].

The BET model improved the Langmuir model by creating a multilayer model with a random distribution of adsorption sites and no longer assuming an ideal gas. This model allows for attraction and adherence between gas molecules and adsorbents that can act as a substrate for multiple adsorption layers. The model is defined by Eq. 3.

$$\frac{V}{V_{mon}} = \frac{cz}{(1-z)(1-z+cz)} \quad (3)$$

where $z = p_0/p$, p is the equilibrium pressure, p_0 is the vapour saturation pressure, V_{mon} is the volume corresponding to the surface being covered by a monolayer, V is the gas volume, and c is a constant [25].

The D-A model has been used to describe micropore volume filling and the solids' energetic heterogeneity with multilayer pores [26], [27]. The fraction of micropore filling θ is defined Eq. 4.

$$\theta = f_i \exp \left[- \left(\frac{A}{E_i} \right)^n \right] = \frac{V_{oi}}{V_i} \exp \left[- \left(\frac{RT \ln(P_{sat} / P)}{E_i} \right)^n \right] \quad (4)$$

where $f_i = V_{oi}/V_i$ is the fraction of occupied adsorption sites located in the micropores with an adsorption characteristic energy E_i , and the adsorption potential is $A = RT \ln(P_0/P)$. The Tóth isotherm is an empirical model built off the Langmuir model that can provide more accurate results at low and high pressures [28], [29]. The fraction of occupied adsorption sites θ is defined Eq. 5.

$$\theta = \frac{K_T p}{[1 + (K_T p)^t]^{\frac{1}{t}}} \quad (5)$$

where K_T and t are equation constants, and p is the equilibrium pressure. When $t = 1$, the Tóth isotherm is identical to the Langmuir isotherm. The value of t describes the heterogeneity of the adsorbent micropores [28], [30]. The adsorption data of this study were fitted to two isotherm models proposed by Tóth and Dubinin–Astakhov (D-A model) with a predictive accuracy of better than 3 %. This study develops the ongoing data set for high-performing activated carbon, its adsorption abilities with differing adsorbents, and an understanding of what deviations are present compared to the widely used adsorption models. This study includes the construction of Tóth isotherms in varying conditions. Building a strong isotherm correlation is desired, with an understanding of the relationship between the pores of the activated carbon sample, operating parameters, and the adsorbent.

2. Material and methods

The activated carbon used in this experiment was Maxsorb II from the Kansai Coke and Chemicals Company. The activated carbon is made from coal, unloaded from large ships at the wharf and transported to the coal storage area by conveyor belt. The coal is blended and crushed, then dry-distilled into coke for steelmaking in the coke ovens. The coke is supplied to Kobe Steel's Kakogawa Works on a 24-hour basis. This company developed and implemented a proprietary automatic coke oven heating control system that reduced coke oven gas (COG) consumption by approximately 5% compared to before it was implemented. This system has been adopted by the New Energy and Industrial Technology Development Organization (NEDO) as an International Demonstration Project on Japan's Energy Efficiency Technologies.

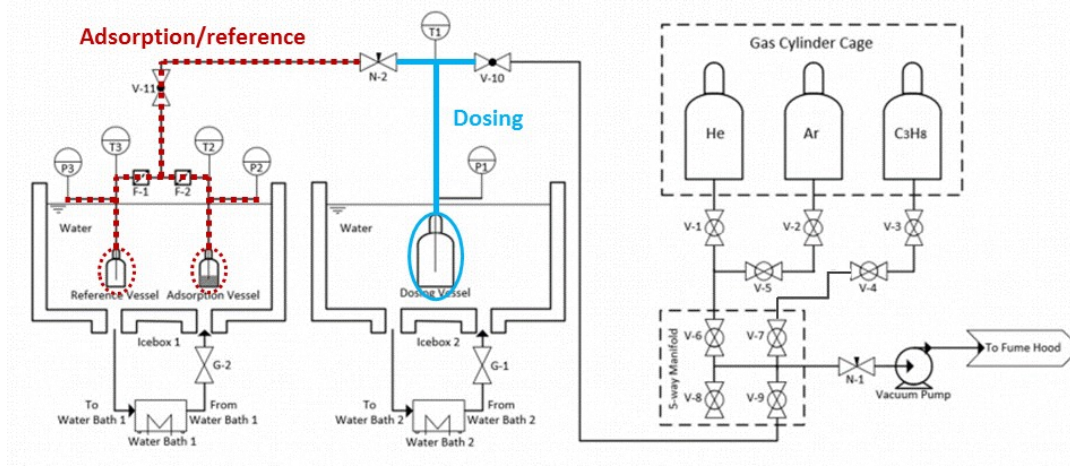


Figure 3. Diagram of the CVVP apparatus

Once the volume of the adsorption/reference section had been determined, the data for the propane isotherms was gathered. At 15°C, the saturation pressure of propane is 7.3 bar, which makes gathering data for an 8-bar run at 15°C impossible as the dosing vessel cannot supply pressure above its saturation pressure to the adsorption vessel.

Another factor in avoiding the 15°C and 8 bar propane run was the risk of unintentionally depositing propane condensation onto the activated carbon. As a safety measure, the cold 15°C dosing vessel was never to be charged with propane at a pressure that could cause condensation, despite the outdoor temperature propane tank being able to supply such a pressure.

Data processing and analysis were carried out during each procedure to verify the success or failure of the experimental runs. All data analysis was done on Microsoft Excel using the data exported from the Keysight BenchVue data logging software. The pressure transducers output their frequency (Hz) data to minimise interference. This is because the data is not readily readable, unlike the RTD data, which directly outputs the temperature at °C. The results could be interpreted once the data had been graphed on comparable scales.

The helium calibration runs were used to calculate the dead volume of the adsorption/reference section. The results from earlier studies were used to acquire the calibrated volume of $V_1=177.1$ cm³ for the dosing vessel [2], [3]. Densities of the gas (in mol/m³) at measured equilibrium temperatures and pressures were obtained using the REFPROP and their molecular weights. The moles of helium that left the dosing vessel during a dosing operation (the short opening of valve N-2) were calculated Eq. 6.

$$n_{dose-Helium} = V_1 \cdot [\rho_{d,i}(T, p_i) - \rho_{d,f}(T, p_f)]_{Helium} \quad (6)$$

where $\rho_{d,i}$ and $\rho_{d,f}$ the dosing vessel helium densities are at equilibrium before and after the dosing procedure.

Summing up, each dose gave a total number of moles in the adsorption/reference section. Since helium is a non-adsorbing gas, all the moles of gas in the adsorption/reference section will be assumed to be in a vapour phase and, therefore, contribute to the state of the gas. Based on this assumption, the volume of the adsorption/reference section V_2 can then be calculated Eq. 7.

$$V_2 = \frac{\sum n_{dose-Helium}}{\rho_{adsorption-Helium}(T, p)} \quad (7)$$

where $\rho_{adsorption-Helium}(T, p)$ is the density of helium in the adsorption vessel for a measured equilibrium temperature and pressure.

Determining the dead volume of the adsorption/reference section allows for the calculation of the propane amount adsorbed onto the activated carbon. The moles of propane that leave the dosing vessel during a dose is calculated Eq. 8.

$$n_{dose-Propane} = V_1 \cdot [\rho_{d,i}(T, p_i) - \rho_{d,f}(T, p_f)]_{Propane} \quad (8)$$

The moles of gas that are in the vapour phase and contribute to the pressure of the adsorption/reference section are calculated Eq. 9.

$$n_{free} = V_2 \cdot \rho_{adsorption-Propane} (T, p) \tag{9}$$

Taking the difference between the total moles of gas that have entered the system and the moles of gas in a vapour phase allows the moles of propane that have been adsorbed onto the carbon to be calculated Eq. 10.

$$n_{adsorbed} = n_{dose-Propane} - n_{free} \tag{10}$$

Calculations of the adsorption isotherm models were based on work done in a similar paper [3]. A Tóth adsorption isotherm model was fitted to the data. The equation used in this analysis calculated the total mass of adsorbed gas per unit mass of activated carbon, slightly different from the equation (5), which calculates the proportion of filled adsorption sites. The specific adsorption capacity of the adsorbent C with units of grams of propane per gram of activated carbon is given Eq. 11.

$$C = \frac{C_{max} k_0 \exp\left(\frac{\Delta h}{RT}\right) p}{\left(1 + \left[k_0 \exp\left(\frac{\Delta h}{RT}\right) p\right]^t\right)^{\frac{1}{t}}} \tag{11}$$

where C_{max} is the maximum specific adsorption capacity of the adsorbent, k_0 is the pre-exponential constant, Δh is the isosteric heat of adsorption, R is the universal gas constant, and t is the dimensionless Tóth constant, which measures the heterogeneity of the adsorbent micropores [3]. T and p are the temperature and pressure at an equilibrium point and the equation parameters C_{max} , k_0 , $\Delta h/R$, and t are fitted to the experimental data.

3. Results and discussion

After the activated carbon successful regeneration, the helium non-adsorbing behaviour was confirmed by the linearity of the dosed moles versus the pressure, with the data shown in Figure 4. The dead volume was measured to be $V_2 = 42.3 \text{ cm}^3$ using equations (6) and (7). The full set of helium equilibrium data points is used to calculate the dead volume and create Figure 4.

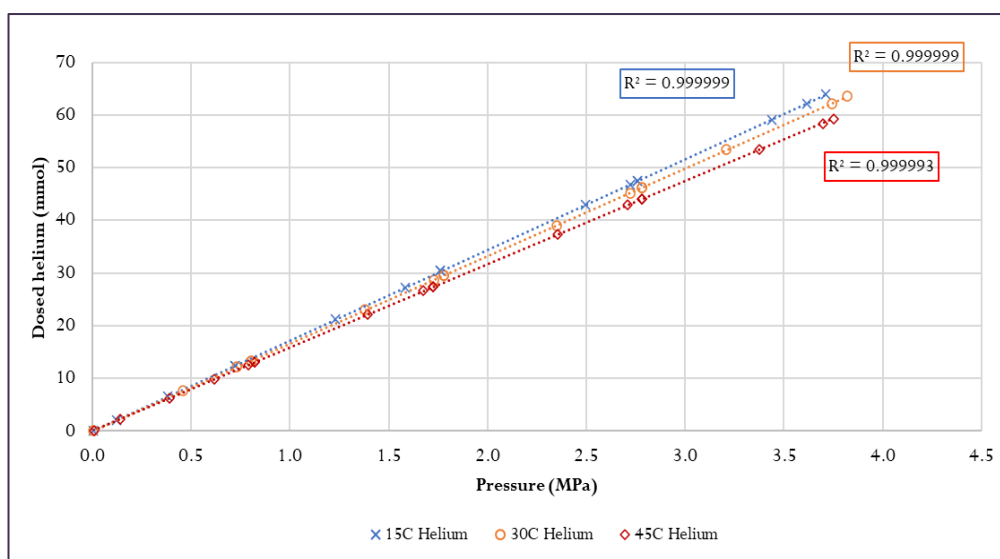


Figure 4. Helium calibration plot

Equations (8), (9), and (10) were used to create the plot for the specific adsorption of propane shown in Figure 5. Propane data at 30°C 8 bar had been gathered but was found to have procedural error and was removed from the data set. The initial behaviour of the data at low pressures is a linear increase of adsorption with pressure, but this then flattens out as the pressure increases. This is typical of activated carbon and fits a Type 1 IUPAC physisorption isotherm, where the initial filling of pores with the adsorbate increases linearly with the pressure but then flattens out as the adsorbent reaches saturation without the pore size to form significant multilayer adsorbates [31]. The experimental data and the fits with the two isotherms in Figure 5 show the deviation plots for the two isotherms. In the D–A isotherm, the parameter designating the thermal expansion of the adsorbed phase-specific volume was used by Rubes et al. [32] and Saha et al. [20]. It is seen that the D–A equation is associated with larger positive deviations than the Tóth equation and negative deviations in the uptake region, indicating that the curvature of the isotherm in the lower temperatures is not exactly reproduced.

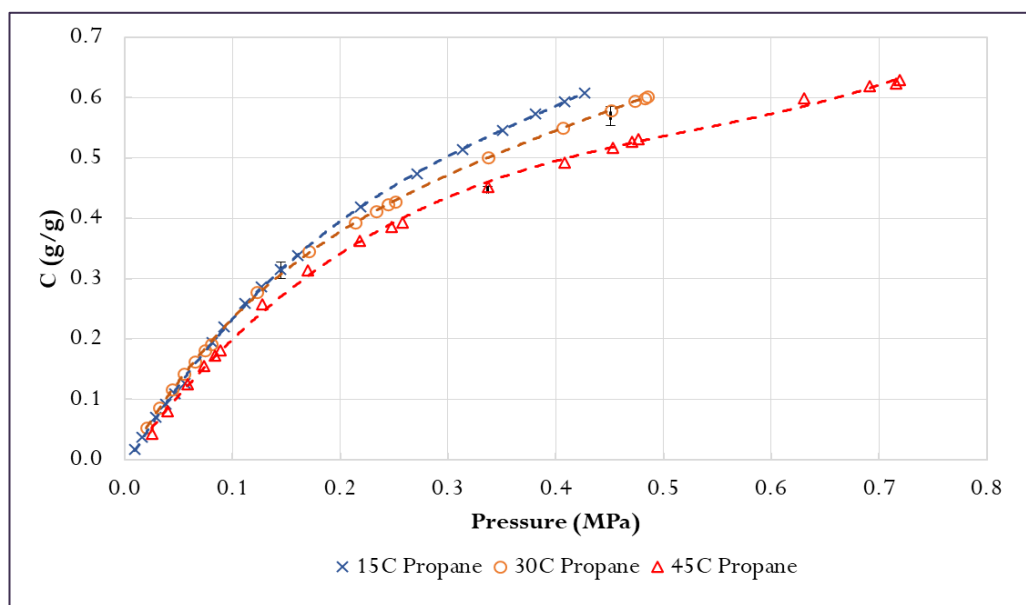


Figure 5. Propane adsorption on activated carbon isotherm plot, with a fitted Tóth isotherm

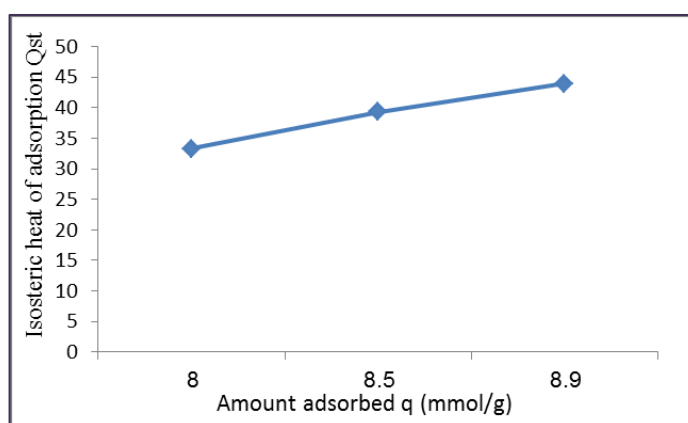


Figure 6. Isothermic heat of adsorption as a function of the amount adsorbed [33]

The isothermic heat of adsorption increased as the adsorption capacity increased, as seen in Figure 6. Significant lateral interactions between adsorbates at adsorbent sites caused this increase. The propane molecules preferentially bind at cage centre sites, followed by adsorption at cage window sites, as explained by Rubes [32]. The adsorption enthalpies rise as propane loading increases because the adsorbates at the cage centre and cage window sites have strong lateral interactions.

When the isosteric heat of adsorption increased with coverage (due to increasing the lateral interaction between adsorbate-adsorbate interactions while decreasing the binding energy between adsorbate molecules and the adsorbent surface), this resulted in a decrease in the number of propane molecules that could be adsorbed and a decrease in the amount of gas delivered at desorption due to more gas molecules remaining in adsorbent sites due to the increased lateral interaction [33].

4. Conclusion

The data and results of this study will provide a valuable addition to the body of knowledge of its larger parent project and assist in future research. The accurate measurement of the dead volume was determined to be $43.3 \pm 0.7 \text{ cm}^3$, and it verified results from previous studies. The dead volume measurement allowed for gathering data on propane adsorption, which was set out at the beginning of the project. Data could be gathered across the full desired range of 2-8 bar pressures and temperatures of 15-45° C. Analysis of the data gave a well-fitted Tóth adsorption isotherm, giving the maximum specific adsorption capacity of the activated carbon to be 2.28 g of propane per gram of activated carbon with a standard error of regression $\hat{\sigma}$ of 0.01 g/g. The accuracy of the data has room for improvement, with one of the eleven propane data runs having a procedural error. In addition, there is an opportunity for enhanced uncertainty analysis if the sensor reading discrepancies can be improved.

Author contribution

Tine Aprianti: Writing – original draft, formal analysis, investigation, resources, data curation, visualisation, and project administration. Harrini Muatiara Hapsari, Debby Yulinar Permata, Selvia Aprilyanti, Kallan Pham, and Justin Sobey: Software, resources, data curation, visualisation, and project administration. Harrini Mutiara Hapsari and Debby Yulinar: Analysis, resources, data curation, visualisation, and project administration. Kandadai Srinivasan: Validation, terminology, writing - review & editing, formal analysis, and supervision. Hui Tong Chua: Conceptualisation, methodology, validation, formal analysis, writing – review & editing, supervision, and funding acquisition.

Funding statement

The research/publication of this article was funded by DIPA of Public Service Agency of Universitas Sriwijaya 2023. SP DIPA-023.17.2.677515/2023, on November 13, 2022. In accordance with the Rector's Decree Number: 0189/UN9.3.1/SK/2023, on April 18, 2023".

Acknowledgements

The authors thank Universitas Sriwijaya and The University of Western Australia for funding and facilitating this research.

Competing interest

We declare that we have no known competing financial interests or personal relationships that could have appeared to influence the work reported in this paper.

References

- [1] P. P. Pandav, S. B. Barve, N. R. Anekar, and S. S. Hatwalane, "Eco-friendly Refrigerants," in *International Conference on Renewable Energy and Sustainable Development, ICRESD 2014* -

- Proceedings*, 2014. https://www.researchgate.net/publication/351710022_Eco-friendly_Refrigerants
- [2] W. Shin, “Experimental Study of Gas Adsorption with Activated Carbon : Constant-Volume-Variable-Pressure Apparatus Design and Helium Calibration,” The University of Western Australia, 2020.
- [3] X. Wang, J. French, S. Kandadai, and H. T. Chua, “Adsorption Measurements of Methane on Activated Carbon in the Temperature Range (281 to 343) K and Pressures to 1.2 MPa,” *J Chem Eng Data*, vol. 55, no. 8, pp. 2700–2706, 2010, <https://doi.org/10.1021/je900959w>
- [4] I. Koutník, M. Vráblová, and J. Bednárek, “Reynoutria japonica, an invasive herb as a source of activated carbon for the removal of xenobiotics from water.,” *Bioresour Technol*, vol. 309, p. 123315, Aug. 2020, <https://doi.org/10.1016/j.biortech.2020.123315>
- [5] D. Lozano-Castello, D. Cazorla-Amorós, and A. Linares-Solano, “Powdered Activated Carbons and Activated Carbon Fibers for Methane Storage: A Comparative Study,” *Energy Fuels*, vol. 16, no. 5, pp. 1321-1328, 2002, <https://doi.org/10.1021/ef020084s>
- [6] R. Rajbhandari, L. K. Shrestha, and R. R. Pradhananga, “Preparation of Activated Carbon from Lapsi Seed Stone and its Application for the Removal of Arsenic from Water,” *Journal of the Institute of Engineering*, vol. 8, no. 1–2, pp. 211–218, Jan. 1970, <https://doi.org/10.3126/jie.v8i1-2.5113>
- [7] A. Mianowski, M. Owczarek, and A. Marecka, “Surface area of activated carbon determined by the iodine adsorption number,” *Energy Sources, Part A: Recovery, Utilization and Environmental Effects*, vol. 29, no. 9, pp. 839–850, Jan. 2007, <https://doi.org/10.1080/00908310500430901>
- [8] T. Aprianti, B. D. Afrah, and T. E. Agustina, “Acid Mine Drainage Treatment Using Activated Carbon Ceramic Adsorbent in Adsorption Column,” *Int J Adv Sci Eng Inf Technol*, vol. 7, no. 4, pp. 1241-1247, 2017. <http://dx.doi.org/10.18517/ijaseit.7.4.2593>
- [9] T. Aprianti, T. I. Sari, F. Hadiah, Y. Utama, and M. Said, “Powdered Activated Carbon (PAC)-Ceramic Composite Adsorbent for Iron and Aluminum Cations Removal from Acid Mine Drainage,” *Journal of Engineering and Technological Sciences*, vol. 54, no. 1, pp. 186-198, 2022, <https://doi.org/10.5614/j.eng.technol.sci.2022.54.1.13>
- [10] T. H. C. Yeo, I. A. W. Tan, and M. O. Abdullah, “Development of adsorption air-conditioning technology using modified activated carbon - A review,” *Renewable and Sustainable Energy Reviews*, vol. 16, no. 5, pp. 3355–3363, Jun. 2012. <https://doi.org/10.1016/j.rser.2012.02.073>
- [11] N. Muttli, S. Jagadeesan, A. Chanda, M. Duke, and S. K. Singh, “Production, Types, and Applications of Activated Carbon Derived from Waste Tyres: An Overview,” *Applied Sciences (Switzerland)*, vol. 13, no. 1. MDPI, Jan. 01, 2023. <https://doi.org/10.3390/app13010257>
- [12] E. N. El Qada, S. J. Allen, and G. M. Walker, “Adsorption of Methylene Blue onto activated carbon produced from steam activated bituminous coal: A study of equilibrium adsorption isotherm,” *Chemical Engineering Journal*, vol. 124, no. 1–3, pp. 103–110, Nov. 2006, <https://doi.org/10.1016/j.cej.2006.08.015>
- [13] T. Aprianti, S. Miskah, R. Moeksin, S. Sisnayati, and S. Nasir, “Pb removal in pulp and paper industry leachate wastewater using activated carbon-ceramic composite adsorbent,” *IOP Conf Ser Earth Environ Sci*, vol. 298, no. 1, 2019, <https://doi.org/10.1088/1755-1315/298/1/012011>
- [14] T. Aprianti, S. Miskah, Selpiana, R. Komala, and S. Hatina, “Heavy metal ions adsorption from pulp and paper industry wastewater using zeolite/activated carbon-ceramic composite adsorbent,” *AIP Conf Proc*, vol. 2014, no. 2018, 2018, <https://doi.org/10.1063/1.5054531>
- [15] T. H. C. Yeo, I. A. W. Tan, and M. O. Abdullah, “Development of adsorption air-conditioning technology using modified activated carbon - A review,” *Renewable and*

- Sustainable Energy Reviews*, vol. 16, no. 5. pp. 3355–3363, Jun. 2012.
<https://doi.org/10.1016/j.rser.2012.02.073>
- [16] P. Sinha, A. Datar, C. Jeong, X. Deng, Y. Chung, and L.-C. Lin, “Surface Area Determination of Porous Materials Using the Brunauer-Emmett-Teller (BET) Method: Limitations and Improvements,” *The Journal of Physical Chemistry C*, vol. 123, no. 33, pp. 20195–20209, 2019, <https://doi.org/10.1021/acs.jpcc.9b02116>
- [17] J. M. Calm and D. A. Didion, “Trade-offs in refrigerant selections: past, present, and future,” *International Journal of Refrigeration*, vol. 21, no. 4, pp. 308–321, 1998, [https://doi.org/10.1016/S0140-7007\(97\)00089-3](https://doi.org/10.1016/S0140-7007(97)00089-3)
- [18] M. Fatouh and M. El Kafafy, “Assessment of propane/commercial butane mixtures as possible alternatives to R134a in domestic refrigerators,” *Energy Convers Manag*, vol. 47, no. 15–16, pp. 2644–2658, Sep. 2006, <https://doi.org/10.1016/j.enconman.2005.10.018>
- [19] A. Chakraborty, B. B. Saha, K. C. Ng, I. I. El-Sharkawy, and S. Koyama, “Thermodynamic property surfaces for adsorption of R507A, R134a, and n-butane on pitch-based carbonaceous porous materials,” *Heat Transfer Engineering*, vol. 31, no. 11, pp. 917–923, Jan. 2010, <https://doi.org/10.1080/01457631003604152>
- [20] B. B. Saha *et al.*, “Isotherms and thermodynamics for the adsorption of n-butane on pitch based activated carbon,” *Int J Heat Mass Transf*, vol. 51, no. 7–8, pp. 1582–1589, Apr. 2008, <https://doi.org/10.1016/j.ijheatmasstransfer.2007.07.031>
- [21] M. Muzic and K. Sertic-Bionda, “Alternative Processes for Removing Organic Sulfur Compounds,” *Chemical and Biochemical Engineering Quarterly*, vol. 27, no. 1, pp. 101–108 2013. <http://silverstripe.fkit.hr/cabeq/assets/Uploads/14.pdf>
- [22] S. Dey and N. S. Mehta, “Automobile pollution control using catalysis,” *Resources, Environment and Sustainability*, vol. 2, p. 100006, Dec. 2020. <https://doi.org/10.1016/j.resenv.2020.100006>
- [23] M. Vigdorowitsch, A. Pchelintsev, L. Tsygankova, and E. Tanygina, “Freundlich isotherm: An adsorption model complete framework,” *Applied Sciences*, vol. 11, no. 17, p. 8078, Aug. 2021, <https://doi.org/10.3390/app11178078>
- [24] I. Langmuir., “The adsorption of gases on plane surfaces of glass, mica and platinum,” *J Am Chem Soc*, vol. 345, no. 9, pp. 1361–1403, 1918. <https://doi.org/10.1021/ja02242a004>
- [25] A. W. Marczewski, “Analysis of Kinetic Langmuir Model. Part I: Integrated Kinetic Langmuir Equation (IKL): A New Complete Analytical Solution of the Langmuir Rate Equation,” *Langmuir*, vol. 26, no. 19, pp. 15229–15238, 2010, <https://doi.org/10.1021/la1010049>
- [26] A. Gil and P. Grange, “Application of the Dubinin-Radushkevich and Dubinin-Astakhov equations in the characterization of microporous solids,” *Colloids Surf A Physicochem Eng Asp*, vol. 113, no. 1, pp. 39–50, 1996, [https://doi.org/10.1016/0927-7757\(96\)81455-5](https://doi.org/10.1016/0927-7757(96)81455-5)
- [27] K. Srinivasan, P. Dutta, K. Ng, and B. Saha, “Calculation of heat of adsorption of gases and refrigerants on activated carbons from direct measurements fitted to the Dubinin-Astakhov equation,” *Adsorption Science and Technology*, vol. 30, no. 7, pp. 549–565, 2012, <https://doi.org/10.1260/0263-6174.30.7.549>
- [28] A. P. Terzyk, J. Chatlas, P. A. Gauden, G. Rychlicki, and P. Kowalczyk, “Developing the solution analogue of the Toth adsorption isotherm equation,” *J Colloid Interface Sci*, vol. 266, no. 2, pp. 473–476, 2003, [https://doi.org/10.1016/S0021-9797\(03\)00569-1](https://doi.org/10.1016/S0021-9797(03)00569-1)
- [29] K. V. Kumar, M. Monteiro De Castro, M. Martinez-Escandell, M. Molina-Sabio, and F. Rodriguez-Reinoso, “A site energy distribution function from Toth isotherm for adsorption of gases on heterogeneous surfaces,” *Physical Chemistry Chemical Physics*, vol. 13, no. 13, pp. 5753–5759, 2011, <https://doi.org/10.1039/c0cp00902d>
- [30] J. Toth, “Uniform Interpretation of Gas/Solid Adsorption,” *Advances in Colloid and Interface Science*, vol. 55, pp. 1–239, 1995, [https://doi.org/10.1016/0001-8686\(94\)00226-3](https://doi.org/10.1016/0001-8686(94)00226-3)

- [31] K. S. W. Sing, “Reporting Physisorption Data for Gas/Solid Systems with Special Reference to the Determination of Surface Area and Porosity (Provisional),” *Pure and Applied Chemistry*, vol. 54, no. 11, pp. 2201–2218, Jan. 1982. <https://doi.org/10.1351/pac198254112201>
- [32] M. Rubes, A. D. Wiersum, P. L. Llewellyn, L. Grajciar, O. Bludský, and P. Nachtigall, “Adsorption of propane and propylene on CuBTC metal-organic framework: Combined theoretical and experimental investigation,” *Journal of Physical Chemistry C*, vol. 117, no. 21, pp. 11159–11167, May 2013, <https://doi.org/10.1021/jp401600v>
- [33] Mohammed Sattar Jabbar and R. Th. A. Alrubaye, “Adsorption Isotherms and Isotheric Heat of Adsorption of Metal Organic Frameworks as Gas Storage for Liquefied Petroleum Gas Vehicle in Iraq,” *Iraqi Journal of Chemical and Petroleum Engineering*, vol. 23, no. 3, pp. 25–34, Sep. 2022, <https://doi.org/10.31699/ijcpe.2022.3.4>